Effect of Time-Varying Moving Structures on the Spatial Accuracy of Five-Axis Machine Tools

Tzu-Chi Chan (tcchan@nfu.edu.tw)
National Formosa University

Jyun-Sian Yang
National Formosa University

Research Article

Keywords: Five-axis machine tool, Finite element method, Modal analysis, Spatial position error analysis, Time-varying moving structure

Posted Date: March 19th, 2021

DOI: https://doi.org/10.21203/rs.3.rs-298304/v1

Abstract

Machine tools are constantly in motion during machining; however, studies have not considered the effect of the dynamic and static characteristics of the machine caused by the movement of the structure over time. In this study, the time-varying moving structure in the spatial coordinate arm is analyzed to improve the spatial accuracy of the motion of a five-axis machine tool in the cutting area. The objective is to design a high-speed five-axis moving-column machine tool and to perform structural analysis of spatial accuracy. We studied the static and dynamic characteristics of a five-axis machine tool, designed and improved its mechanical structure, and optimized its structural configuration. With further analysis, the entire machine structure was enhanced to improve its static and dynamic characteristics. The static and dynamic characteristics of the machine structure were found to directly affect its processing performance and the precision of the workpiece machined by the tool. Through this study, the design technology for speed, accuracy, and surface roughness of the machine tool was further improved.

Introduction

A machine tool is a positive representative of national industrialization. Traditional machine tool design and manufacturing results are inconsistent, resulting in waste materials and increased costs. Therefore, this study uses a five-axis machine tool as a development objective and introduces computer-aided engineering analysis technology. We hope to decrease the uncertainty associated with machine development and increase the accuracy of the machine tools.

Wu et al. [1] presented the mechatronic modeling and forced vibration of a 2- degrees of freedom (DOF) parallel manipulator in a 5-DOF hybrid machine tool that was investigated. The results showed that a higher bandwidth and lower structural frequency lead to more interactions between the mechanical and control subsystems. Gegg et al. [2] investigated experimental studies showing that the superposition of axial ultrasonic vibrations in the milling operation improved the process by reducing cutting forces and enhancing surface finish. Whalley et al. [3] investigated the resonance conditions and the identification of adverse cutting frequencies at which dynamic amplification and system time-domain performance were determined. Zhou et al. [4] investigated and proposed a new method for modeling and predicting thermal deformation of ball screws rather than relying on data from temperature sensors and real-time data from computer numerical controls. Vivek et al. [5] presented particle-reinforced polymer composites with different compositions, which were studied for machine tool structures.

The impact of the particle composition (polymer resin type and ratio) on the damping ratio and elastic modulus was investigated by conducting an impact hammer vibration test. Nagesha et al. [6] investigated a new method that integrates the principle of a shock absorber with a machine using a receiver coupling method to prioritize asymmetric dynamics. Chen et al. [7] studied the essential intelligent machine tool characteristics needed to acquire and accumulate knowledge through learning and to propose original key supporting technologies. Bustillo et al. [8] proposed a new method for the design of machines with ultralight structural components and the development of countermeasures

against productivity loss caused by lightweight machines. Ding et al. [9] changed the 3D topology design optimization problem to a 2D problem to optimize the layout of the stiffener plate in the bed. He et al. [10] used a low carbon footprint as an important benchmark for determining the product performance.

Gu et al. [11] developed a series of compensation methods and used the measurement results of one or more identical machined parts to compensate for five-axis machine errors. Li et al. [12] used the principle of self-optimal growth of plant branches in nature to design the internal stiffener layout of large machine tools. Cai et al. [12] investigated the existing growth algorithm and suggested possible improvements to validate the effectiveness of the method. Luo et al. [13] studied the key machine elements and machine design procedures of ultra-precision machine tools. Bossmanns et al. [14] presented a systematic method to assist in the conceptual design of a high-speed machining– machine tool interface.

Based on the proposed conceptual design method, two realization concepts for high-speed end mills were developed. Bohez [15] classified possible conceptual designs and actual existing implementations based on theoretically possible combinations of DOF. Some useful quantitative parameters, such as the workspace utilization factor, machine tool space efficiency, orientation space index, and orientation angle index, were defined. Praniewicz et al. [16] recommended that these motion error constants can be derived from the eccentricity values obtained in the 3-axis simultaneous test of a bench 5-axis machine tool. Shen et al. [17] proposed a new structural dynamic design optimization method for a holistic machine tool.

Mahdavinejad [18] presented a dynamic model of a lathe that analyzed the instability of the machining process. This was provided by the finite element method and the ANSYS software. The structure of the machine and the combination of the workpiece and tool were considered, and a modal test was performed to evaluate the model.

The machine tool constantly moves during machining, and previous studies have not considered the influence of the movement of the structure on the dynamic and the static characteristics of the structure. Geometric errors are generated, and the dynamic behavior changes with the machine weight because of its moving structure in the spatial position. In this study, the time-varying structural performance was analyzed in the spatial coordinate arm to improve the spatial accuracy of the motion of a five-axis machine tool in the cutting area. Because of the structural deformation and spatial geometric errors caused by the moving structure of the machine, relative deformation errors can be evaluated through the spatial position error compensation analysis to improve the accuracy of the machine. We designed a five-axis machine and, in addition to considering the stability of the machine, an improved machine configuration was considered. Finally, the finite element method was used for static and dynamic analyses, and static stiffness analysis was used to verify the improved results.

Materials And Methods

The purpose of this research was to design a five-axis machine tool and perform a structural optimization analysis. The finite element method was used to analyze and compare the performance changes and

optimize the machine design. A flowchart of the analysis and experimental architecture is shown in Fig. 1.

In this study, a high-order five-axis machine tool was designed, as shown in Fig. 2, and the machine structure was optimized and analyzed. The main structural material is gray cast iron, S40C medium carbon steel, and tungsten carbide; a finite element model was then established, and the boundary interface parameters for finite element analysis were set to explore the structural characteristics, as shown in Fig. 3.

The machine comprises numerous parts. The contact between the slider and slide rail was simulated with a spring. The rigidity of the spring was set to 1,960 N/μm, and the gravitational acceleration was 9.8 m/s^2. The number of nodes was 1,101,810, and the number of elements was 713,791. The model is shown in Fig. 4, and the material properties are listed in Table 1.

Table 1 Material properties

Gray cast iron	
Density (kg/m^3)	7,200
Young's modulus (pa)	1.24e+11
Poisson's ratio	0.3
S40c medium carbon steel	
Density (kg/ m^3)	7850
Young's modulus (pa)	2e+11
Poisson's ratio	0.28
Tungsten carbide	
Density (kg/ m3)	15,000
Young's modulus (pa)	5.5e+11
Poisson's ratio	0.28

Results

During machining, the simulation machine was subjected to a force of 1,000 N, which was applied to the tool tip point in the X-direction. The analysis results show that the major deformations of the main shaft and screw are relatively large, with the maximum deformation being 33.2 μm. The results of the static stiffness analysis are shown in Fig. 5. Concurrently, we also carried out static rigidity experiments. The

results of the experiment and comparison of the analysis results are shown in Figs. 6 and 7, respectively. The static stiffness analysis result was 30.0 N/μm, and the test result was 26.5 N/μm. The difference between the test and analysis results is 11.6%. Owing to the interface nonlinearity, the result was within the error range.

A finite element analysis machine was used to analyze the dynamic machine characteristics, and the analysis frequency setting range was 1–1,000 Hz. From the modal analysis results, it can be seen that the frequencies are 97.5, 110.4, 115.6, and 129.6 Hz, as listed in Table 2. The error of each modal analysis and experiment was within 8.1%.

Table 2 Modal analysis and model testing

Modal analysis frequency (Hz)	Model shape	Model testing frequency (Hz)	Error (%)
97.5	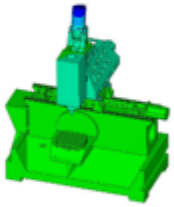	104.0	+6.6
110.4		118.0	+6.8
115.6	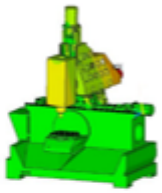	125.0	+8.1
129.6		133.0	+2.6

Discussion

4.1 Effect of moving structure on dynamic structure performance in different locations

This study determined the frequency changes at three different locations. Position A is the leftmost point of X, the foremost point of Y, and the uppermost point of Z on the five-axis machine, and the frequencies are 43.9, 60.4, 89.3, and 105.4 Hz, as shown in Fig. 8. Position B is the center of X, the center of Y, and the center of Z, and the intermediate mode frequencies are 45.6, 70.5, 82.5, and 103.4 Hz, as shown in Fig. 9. Position C is the rightmost point of X, the hindmost point of Y, the lowest point of Z, and the mode frequencies are 60.2, 95.9, 98.4, and 129.6 Hz, as shown in Fig. 10. The machine's modal frequency changes at different positions are shown in Fig. 11.

4.2 Effect of moving structure on static structure accuracy

In the X-, Y-, and Z-axis moving distance ranges, we observe the X, Y, and Z axes separately, as shown in Figs. 12–14. The amount of relative deformation between the tool and the work platform, along with the deformation, changes at different processing points; we can see that the most significant difference is in the Y-axis. Because the machine has a single-axis oscillating mechanism, the magnitude of the relative deformation of the Y-axis is 8.9 μm.

Because the machine's center of gravity does not deviate significantly when the rotating shaft moves, the amount of space deformation remains relatively unchanged at different angles. Therefore, when the machine is cutting, the accuracy of the machine constantly changes. From the results, it can be seen that the rotary table is −30, 30, 45, 60, and 90 °, and the variability is not significantly different. The amount of change is within 1 μm, as shown in Fig. 15.

Conclusion

Currently, because of rapid industrial development and improved machine accuracy and efficiency, the configuration requirements for the structural design of five-axis machines and the design and analysis of structural parts are extremely important. To achieve overall machining accuracy, this research used finite element analysis to analyze the entire machine structure, including static and dynamic analysis, for improving the machine design method.

In this study, the simulation machine was operated under actual processing conditions. In addition, a static analysis was performed when a force of 1,000 N was applied to the blade tip in the X-axis direction. The maximum deformation obtained was 33.2 μm. The difference between the test and analysis results was within 11.6 %. Owing to the nonlinearity of the interface, the result was within the error range. The error of each modal analysis and experiment was within 8.1%.

In the X-, Y-, and Z-axis moving distance ranges, we can observe that the amount of relative deformation between the tool and the work platform changes at different points. Furthermore, we discuss a

comparison of the dynamic machine structure trends when machine components are in different positions. As the machine tool is constantly in motion during machining, geometric errors are generated, and the dynamic behavior changes with machine weight owing to its moving structure in the spatial position.

Declarations

-Ethical Approval: This paper does not contain any studies with human participants or animals performed by any of the authors.

-Consent to Participate: This paper does not contain any studies with human participants performed by any of the authors.

-Consent to Publish: All authors have read and agreed to the published version of the manuscript.

-Authors Contributions: Formal analysis, writing and funding acquisition, Tzu-Chi Chan; software and data curation, Jyun-Sian Yang.

-Funding: This research was funded by Ministry of Science and Technology of the R.O.C., grant number MOST 107-2218-E-150-005-MY3 and MOST 109-2622-E-150-014).

-Competing Interests: The authors have no conflicts of interest to declare that are relevant to the content of this article.

-Availability of data and materials: The authors confirm that the data supporting the findings of this study are available within the article and its supplementary materials.

Acknowledgments

The authors are greatly indebted to the Ministry of Science and Technology of the Republic of China for supporting this research (grant numbers MOST 107-2218-E-150-005-MY3 and MOST 109-2622-E-150-014).

Conflicts of Interest: No conflict of interest exists in the submission of this manuscript, and the manuscript is approved by all authors for publication.

References

1. Wu J, Yu G, Gao Y, Wang L (2018) Mechatronics modeling and vibration analysis of a 2-dof parallel manipulator in a 5-dof hybrid machine tool. Mech Mach Theor 121:430–445. https://doi.org/10.1016/j.mechmachtheory.2017.10.023
2. Gegg BC, Suh S, Luo AC (2010) Modeling and theory of intermittent motions in a machine tool with a friction boundary. J Manuf Sci Eng 132(4). https://doi.org/10.1115/1.4001643

3. Whalley R, Abdul-Ameer AA, Ebrahimi KM (2011) The axes response and resonance identification for a machine tool. Mech Mach Theor 46(8):1171–1192. https://doi.org/10.1016/j.mechmachtheory.2011.02.012
4. Zhou H, Hu PC, Tan H, Chen J, Liu G (2018) Modelling and compensation of thermal deformation for machine tool based on the real-time data of the CNC system. Procedia Manuf 26:1137–1146. https://doi.org/10.1016/j.promfg.2018.07.150
5. Vivek A, Holla V, Krupashankara MS, Vignesh A, Kulkarni P (2018) Effect of improving damping ratio on surface finish by filling particulate reinforced polymer composites in machine tool structures. Mater Today Proc 5(5):13664–13673. https://doi.org/10.1016/j.matpr.2018.02.203
6. Nagesh S, Law M (2019) Machine tool design with preferentially asymmetrical structures to improve dynamics and productivity. Procedia CIRP 79:592–595. https://doi.org/10.1016/j.procir.2019.02.086
7. Chen J, Hu P, Zhou H, Yang J, Xie J, Jiang Y, Gao Z, Zhang C (2019) Toward intelligent machine tool. Engineering 5(4):679–690. https://doi.org/10.1016/j.eng.2019.07.018
8. Bustillo A, Oleaga I, Zulaika JJ, Loix N (2015) New methodology for the design of ultra-light structural components for machine tools. Int J Comput Integr Manuf 28(4):339–352. https://doi.org/10.1080/0951192X.2014.900871
9. Ding X, Chen Y, Liu W (2010) Optimal design approach for eco-efficient machine tool bed. Int J Mech Mater Des 6(4):351–358. https://doi.org/10.1007/s10999-010-9142-2
10. He B, Tang W, Huang S, Hou S, Cai H (2016) Towards low-carbon product architecture using structural optimization for lightweight. Int J Adv Manuf Technol 83(5–8):1419–1429. https://doi.org/10.1007/s00170-015-7676-z
11. Gu J, Agapiou JS, Kurgin S (2017) Error compensation and accuracy improvements in 5-axis machine tools using the global offset method. J Manuf Syst 44:324–331. https://doi.org/10.1016/j.jmsy.2017.04.015
12. Li B, Hong J, Liu Z (2014) Stiffness design of machine tool structures by a biologically inspired topology optimization method. Int J Mach Tool Manuf 84:33–44. https://doi.org/10.1016/j.ijmachtools.2014.03.005
13. Luo X, Cheng K, Webb D, Wardle F (2005) Design of ultraprecision machine tools with applications to manufacture of miniature and micro components. J Mater Process Technol 167(2–3):515–528. https://doi.org/10.1016/j.jmatprotec.2005.05.050
14. Bossmanns B, Tu JF (2002) Conceptual design of machine tool interfaces for high-speed machining. J Manuf Process 4(1):16–27. https://doi.org/10.1016/S1526-6125(02)70130-8
15. Bohez EL (2002) Five-axis milling machine tool kinematic chain design and analysis. Int J Mach Tool Manuf 42(4):505–520. https://doi.org/10.1016/S0890-6955(01)00134-1
16. Praniewicz M, Kurfess TR, Saldana C (2019) Error qualification for multi-axis BC-type machine tools. J Manuf Syst 52:211–216. https://doi.org/10.1016/j.jmsy.2019.03.004
17. Shen L, Ding X, Li T, Kong X, Dong X (2019) Structural dynamic design optimization and experimental verification of a machine tool. Int J Adv Manuf Technol 104:3773–3786.

https://doi.org/10.1007/s00170-019-04049-7

18. Mahdavinejad R (2005) Finite element analysis of machine and workpiece instability in turning. Int J Mach Tool Manuf 45(7–8):753–760. https://doi.org/10.1016/j.ijmachtools.2004.11.017

Figures

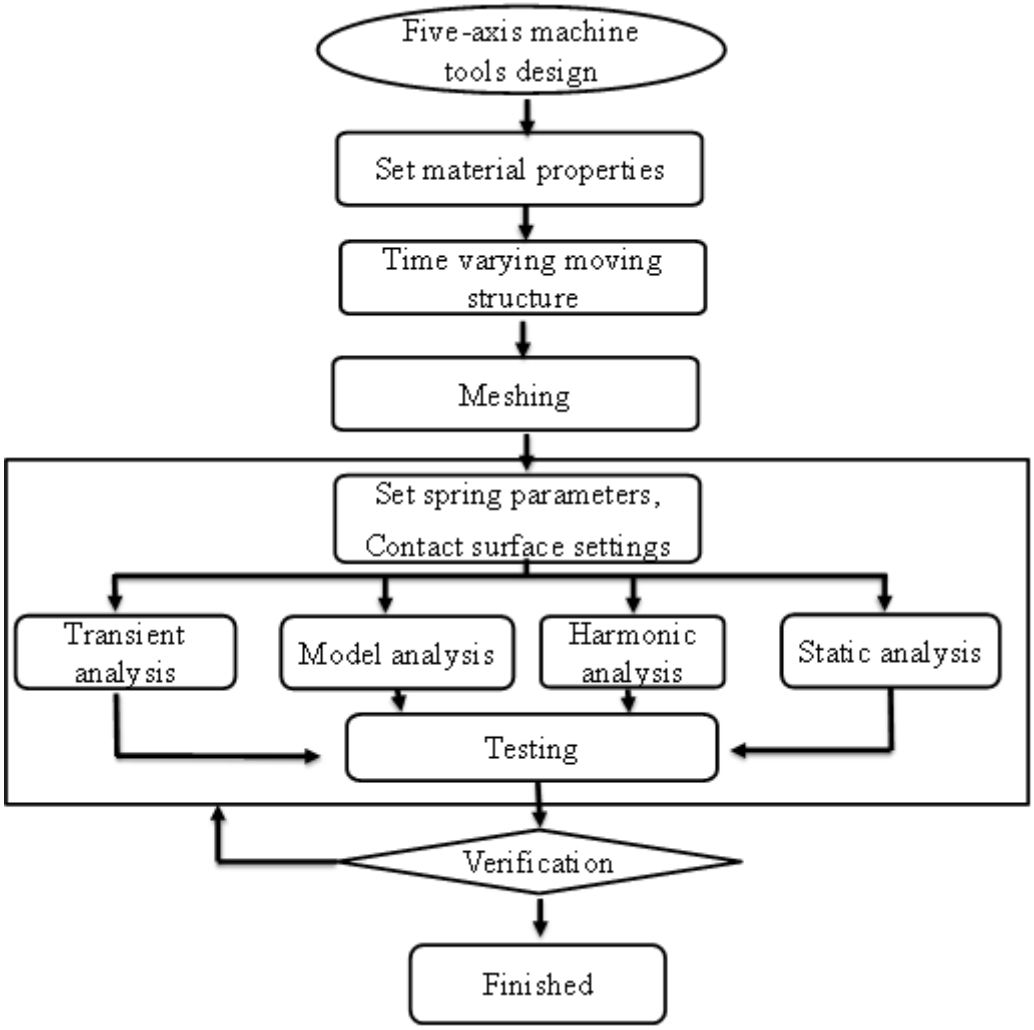

Figure 1

Analysis and experimental architecture flowchart

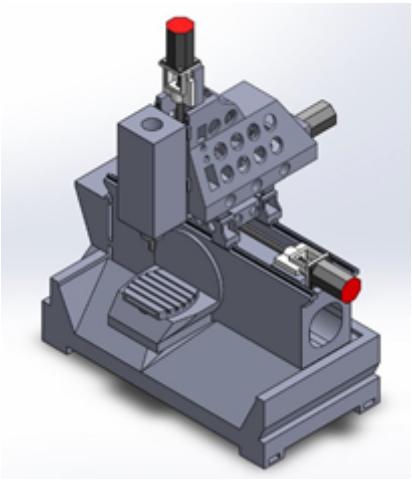

Figure 2

Designed machine model

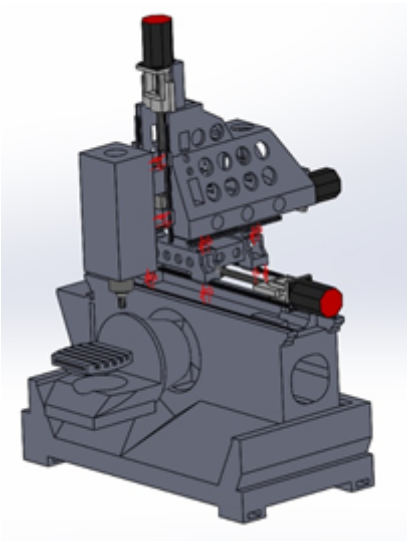

Figure 3

Spring damper boundary conditions

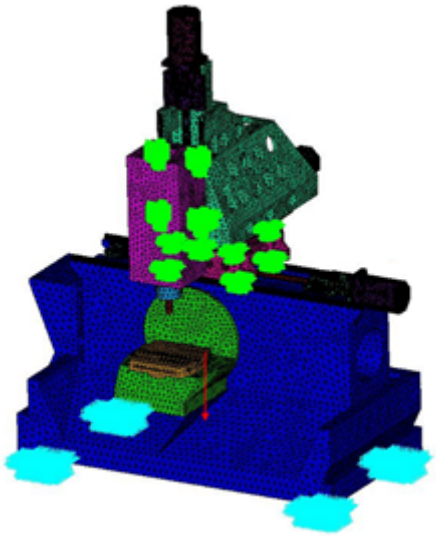

Figure 4

Finite element model of the horizontal machine tool

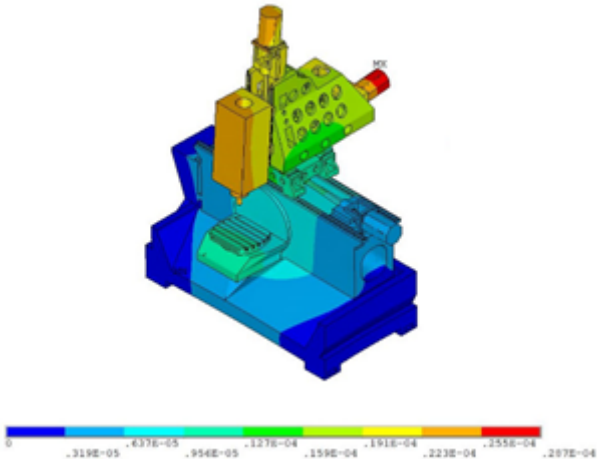

Figure 5

Static rigidity analysis of the horizontal machine tool

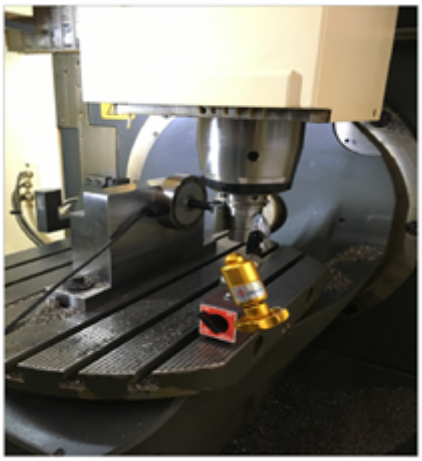

Figure 6

Static stiffness experiment

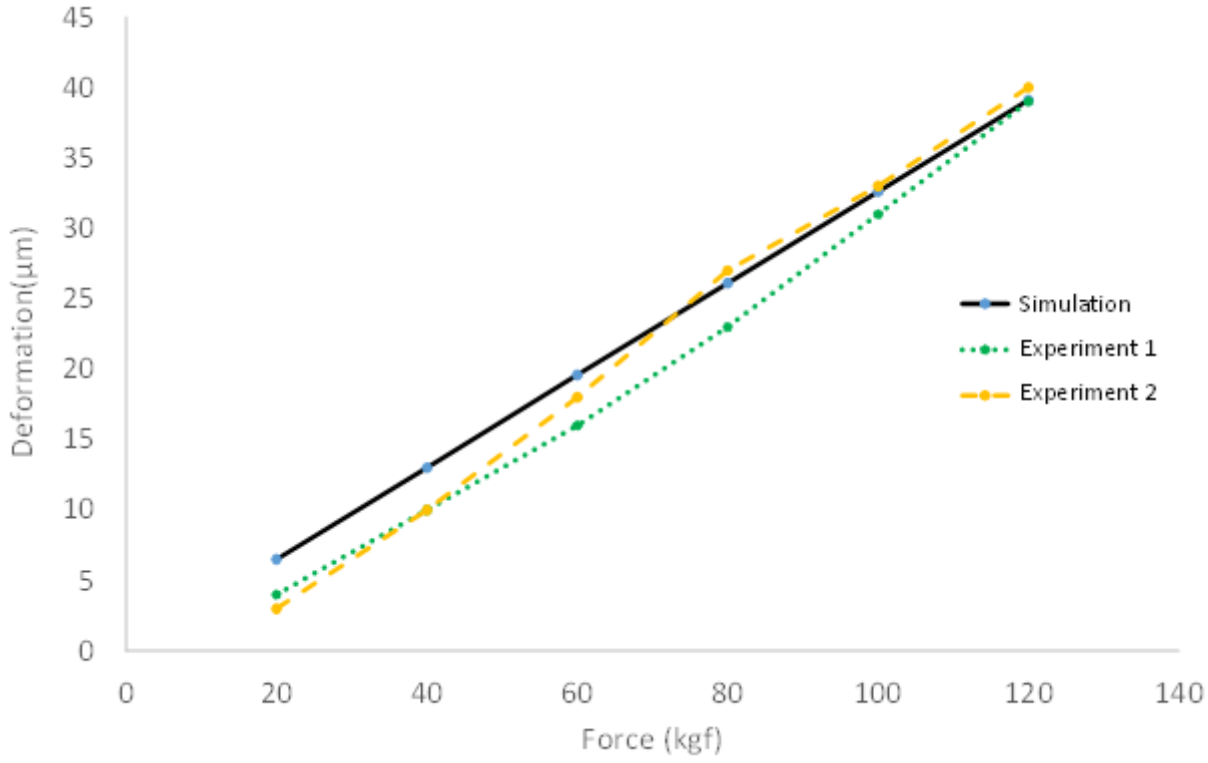

Figure 7

Static stiffness simulation and experiment comparison

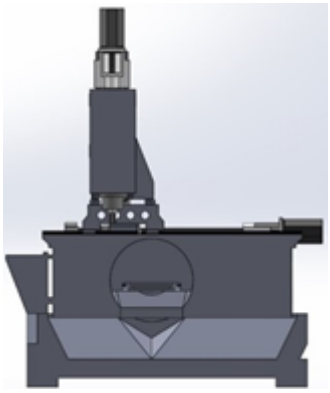

Figure 8

Five-axis machine tool in position A

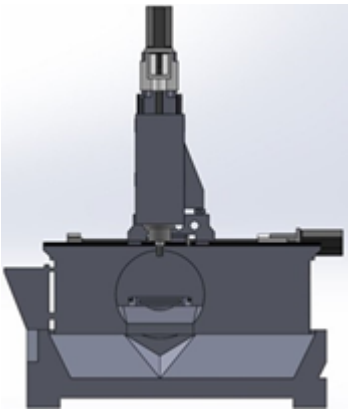

Figure 9

Five-axis machine tool in position B

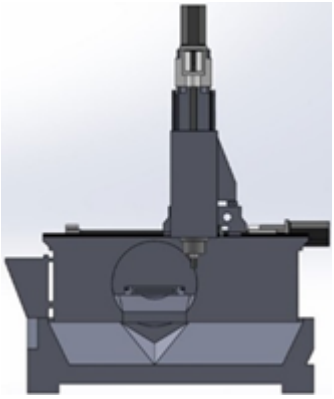

Figure 10

Five-axis machine tool in position C

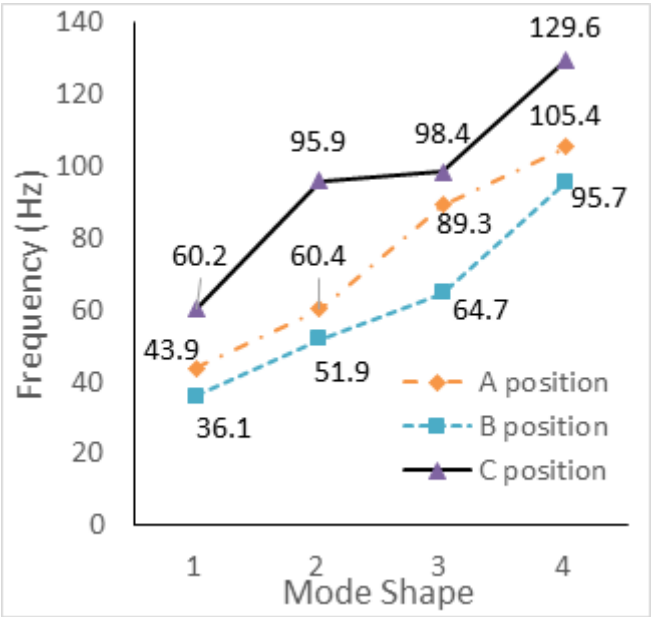

Figure 11

Modal frequency changes of the machine in different positions

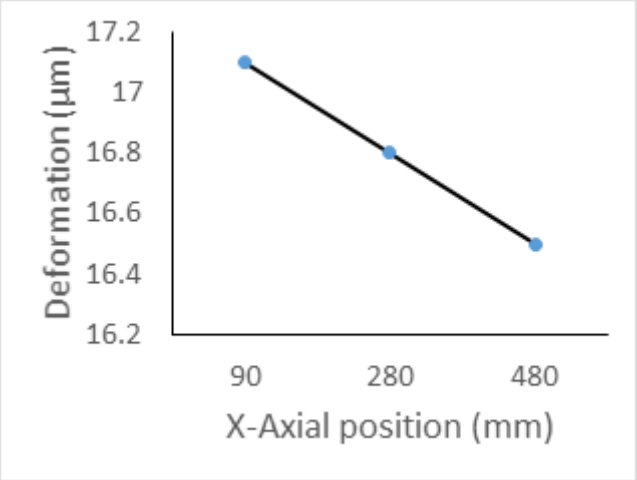

Figure 12

X-axis relative change trend graph

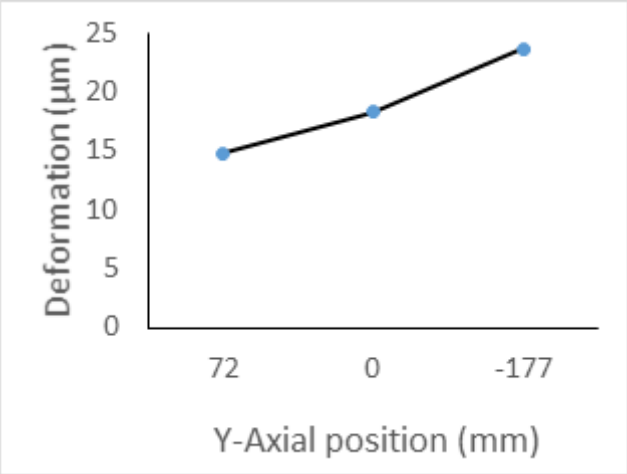

Figure 13

Y-axis relative change trend graph

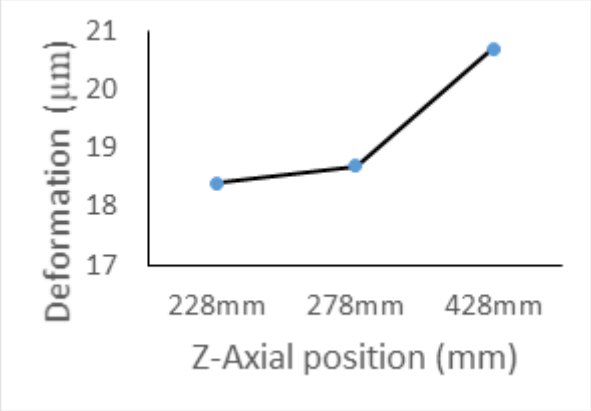

Figure 14

Z-axis relative change trend graph

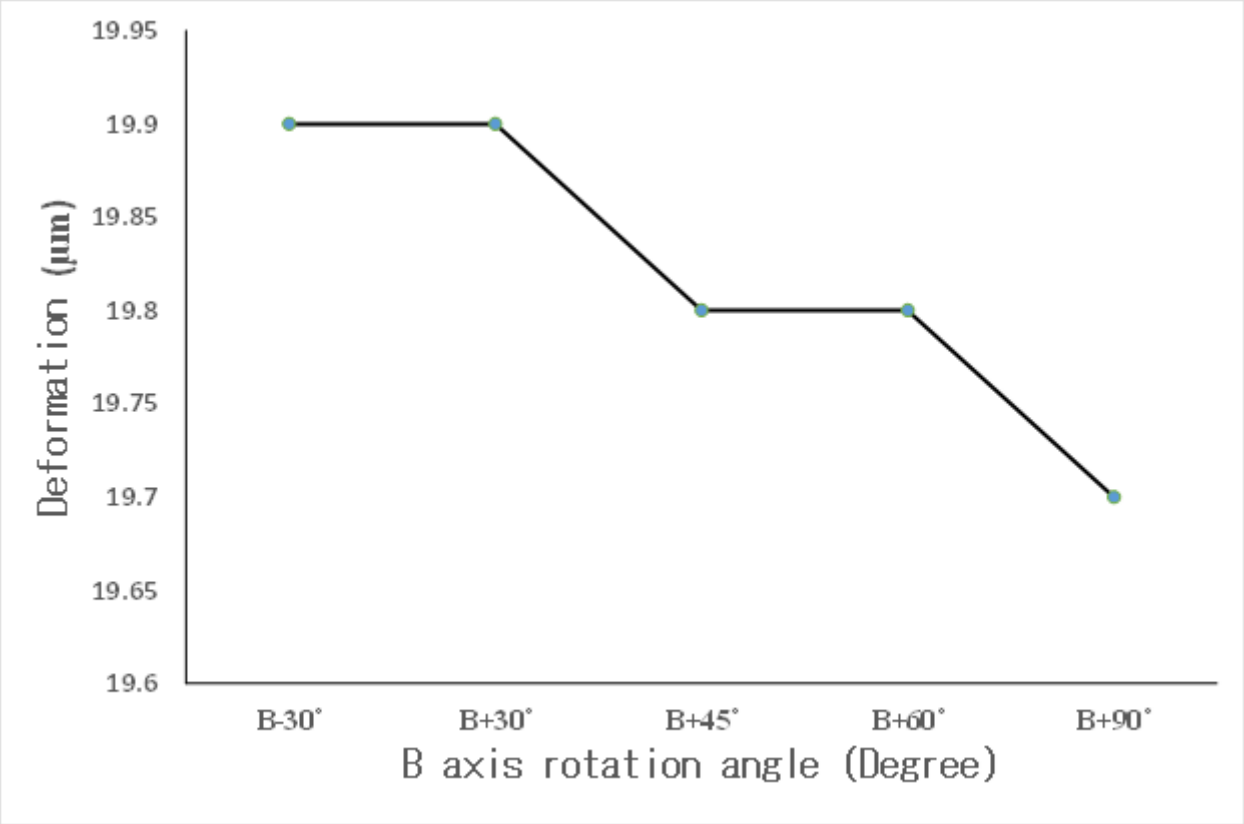

Figure 15

Relationship between B-axis rotation angle and deformation